

50 Gb/s Transmission using OSSB-MultiCAP Modulation and a Polarization Independent Coherent Receiver For Next-Generation Passive Optical Access Networks

Miguel Barrio , David Izquierdo , José Antonio Altabás, and Ignacio Garcés 

Abstract—In this paper, a spectrally efficient version of multi-band Carrierless Amplitude Phase modulation (MultiCAP) based on Optical Single-Sideband (OSSB) techniques is proposed for its use in high capacity access links. The proposed system consists of four 2.5 GBd OSSB-MultiCAP bands with quadrature amplitude modulation and uses an insensitive polarization receiver to avoid optical polarization issues and adjustments at the receiver side. This scheme has been experimentally evaluated and can provide an aggregated transmission rate of 50 Gb/s over 50 km of standard single mode optical fiber using only 10G electronic and photonic devices in C-band with a sensitivity of -23.2 dBm and a measured optical power budget of 25.2 dB. 40 Gb/s transmission over 50 km with a sensitivity of -27.5 dBm and a measured power budget of 32.5 dB is also demonstrated.

Index Terms—Access networks, multiband carrierless amplitude phase modulation, optical single sideband modulation, passive optical networks, polarization independent receiver.

I. INTRODUCTION

PASSIVE optical access networks (PONs) play a fundamental role in home and office high bandwidth communications today. Commercial solutions such as GPON, XG-PON or EPON provide links up to 10 Gb/s shared by several users by time division multiplexing (TDM) techniques. New time and wavelength division multiplexing (TWDM) standards, as NG-PON2 [1], offering downlink bit rates of 4×10 Gb/s, are expected to be deployed in the short term [2]. However, future optical access

networks will have to support high-resolution video and game distribution, cloud computing and storage capabilities, massive IoT applications and signals from countless 5G fronthaul links [3]. In consequence, they will need much more available bandwidth while keeping high optical power budgets at a cost as low as possible. Future PONs are then expected to operate at high bitrates and likely use Wavelength Division Multiplexing (WDM) or even Ultra Dense WDM (UDWDM) approaches to increase the overall provided bandwidth. The spectral efficiency of the transmitted signals and the flexibility of the network will be two key features to address in such future PONs due to the necessity to operate in a heterogeneous environment with many different services and users while coexisting with already installed PONs. Network flexibility would enable the possibility of providing bandwidth for a certain user or service in an adaptive way resulting in a more efficient use of the network resources.

High bit rate (~ 50 Gb/s) single wavelength links are expected to play a role in next generation PONs both as a first step from 10 Gb/s transmission and as the basis for future WDM solutions [2], [4]. Some approaches, mainly based on PAM4 modulation, are based on 25 GHz electrical bandwidth components, which are still expensive for both photonics and RF components, and present limited optical power budgets and reach [5]. Several works have explored different techniques to achieve high bit rate links using ~ 10 GHz electrical bandwidth components [6], [7]. The main goal is to increase the bit count per Hz, so most of the proposals use Optical Frequency Division Multiplexing (OFDM), Discrete Multitone (DMT), SubCarrier Multiplexing (SCM) or MultiCAP modulation schemes to make use of their bit loading capabilities. Among them, OFDM, DMT and SCM suffer high Signal-to-Signal Beat Interference (SSBI) due to their multicarrier nature [8], whereas CAP or MultiCAP solutions can handle better a tradeoff between spectral efficiency, number of channels and interference between bands [9].

Intensity Modulation/Direct Detection (IM/DD) schemes are preferred for PON architectures, as they are cheaper and simpler than coherent approaches nowadays. However, for IM/DD systems at high bandwidths the transmitted signals suffer from chromatic dispersion impairments, such as power fading at some frequencies when propagating through relatively

Manuscript received December 3, 2020; revised March 29, 2021 and May 18, 2021; accepted June 15, 2021. Date of publication June 28, 2021; date of current version September 18, 2021. This work was supported in part by the Diputación General de Aragón under Grant T20_20R and in part by the Spanish MINECO Project FOANT (TEC2017-85752-R), co-funded by FEDER. (Corresponding author: Miguel Barrio.)

Miguel Barrio and Ignacio Garcés are with Photonic Technologies Group (GTF), Aragon Institute of Engineering Research (I3A), Universidad de Zaragoza, 50018 Zaragoza, Spain (e-mail: miguel@unizar.es; ngarcés@unizar.es).

David Izquierdo is with Photonic Technologies Group (GTF), Aragon Institute of Engineering Research (I3A), Universidad de Zaragoza, 50018 Zaragoza, Spain, and also with Centro Universitario de la Defensa (CUD), 50090 Zaragoza, Spain (e-mail: d.izquierdo@unizar.es).

José Antonio Altabás is with Bifrost Communications, Scion DTU, DK-2800 Kgs Lyngby, Denmark (e-mail: jan@bifrostcommunications.com).

Color versions of one or more figures in this article are available at <https://doi.org/10.1109/JLT.2021.3092951>.

Digital Object Identifier 10.1109/JLT.2021.3092951

short distances of optical fiber. This distance is even shorter for higher bandwidths as the ones needed for 50 Gb/s PAM4 based architectures. This problem can be avoided using full coherent reception or Optical Single Sideband (OSSB) modulation as proposed in [10], [11], although they usually present low sensitivities. There has also been interest in the use of Kramers-Kronig receivers [12] as a mean to obtain a native Single Sideband (SSB) modulation and reception, but many of them use multicarrier modulation schemes and require a high Carrier to Signal Power Ratio (CSPR) [13]. OSSB signals also present a narrower spectrum, which may be of interest for UDWDM architectures or applications where there is a restriction in the available spectrum. Moreover, unless Avalanche Photodiodes (APD) are used, DD sensitivities are too small for high bit rate PON applications, so coherent or quasicohherent receivers are getting attention lately [14], [15].

Coherent receivers present higher sensitivities and can handle the power fading issue by means of digital signal processing (DSP). The backwards of coherent receivers are mainly related to polarization management, complex digital signal processing and higher cost. However, we think that coherent PONs will play a fundamental role in optical access in the medium term because of their higher sensitivities, their capacity to handle a multiwavelength environment without filtering and the possibility to integrate the receiver components in the future.

In this work, we will use MultiCAP modulation as well as an optical Hilbert transformed OSSB scheme for the transmission of 40 and 50 Gb/s signals. This scheme takes advantage of spectral and energy efficiency, power and bit loading capabilities and flexibility of the MultiCAP modulation while maintaining a low electrical and optical spectral bandwidth of 11.25 GHz that can be generated using 10G devices. At the receiver side, we use a heterodyne polarization insensitive coherent scheme that will boost the sensitivity of the receiver and eliminate the use of both optical amplification and tunable optical filters in a WDM system. To the best of our knowledge this is the first time a MultiCAP OSSB signal has been used in combination with a polarization independent coherent receiver for the transmission of a 50 Gb/s downstream signal. The use of the OSSB modulation permits to maintain an electrical 11.25 GHz bandwidth despite we are using heterodyne detection, allowing the use of 10G electronics in both, transmitter and receiver side. The used insensitive polarization receiver [16] allows to avoid optical polarization issues and adjustments at the receiver side without complex polarization-time coding techniques such as Alamouti coding [17] and it has been recently used as a 25 Gb/s quasicohherent receiver for links up to 40 km [18]. Using this scheme in this work we will study the transmission of OSSB-MultiCAP downstream signals through 50 km of Standard Single Mode Fiber (SMF). A study of the technology used for the upstream channel is out of the scope of this work. In any case, the same laser used as LO can be used as the upstream source by using an external phase modulator [19], EAM [20], or even a SOA [21]. In a common PON scenario, and taking into account the high bit rate, OSSB modulation and link length of the downstream channel, the upstream transmission may present a lower bandwidth (about 20 Gb/s if we use a 10 Gbd PAM4 signal).

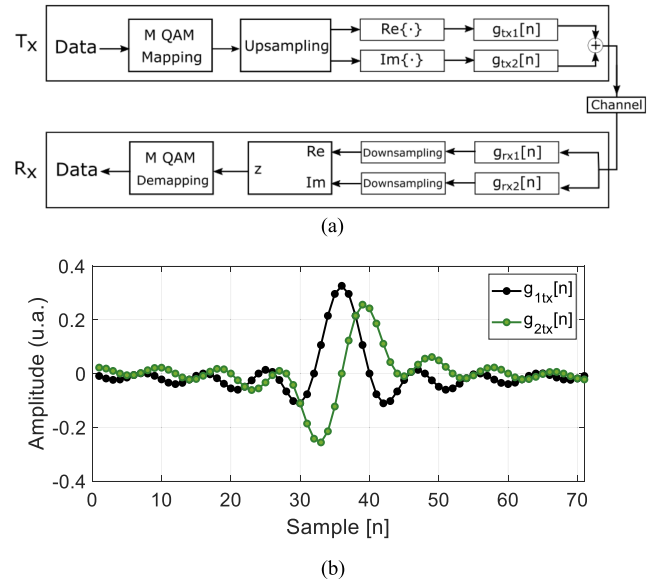


Fig. 1. CAP modulation scheme (a) and impulse response of a pair of orthogonal CAP filters (b) for a 2.5 Gbaud transmission with $\beta = 0.1$. The central frequency of the filter is 1.25 GHz for a sampling rate of $F_s = 20$ GSa/s.

II. SINGLE-SIDEBAND MULTIBAND CARRIERLESS AMPLITUDE PHASE MODULATION

This section provides a short discussion of Carrierless Amplitude Phase (CAP), multiband Carrierless Amplitude Phase (MultiCAP) and Single Sideband (SSB) modulations before presenting its combined use in the Optical Single Sideband multiband Carrierless Amplitude Phase modulation (OSSB-MultiCAP). We use the term OSSB instead of SSB to emphasize that the technique is applied in the optical domain.

A. Carrierless Amplitude Phase Modulation

CAP is a modulation technique similar to quadrature amplitude modulation (QAM) in the sense that two data streams are multiplexed in two orthogonal components, namely the In-phase (I) and Quadrature (Q) components. While in QAM two orthogonal carriers with the same frequency are modulated, CAP uses two orthogonal filters to obtain the two orthogonal components [22]. These filters are the result of the multiplication of a pulse-shaping filter with two orthogonal carriers. The most common pulse-shaping filter is the root-raised-cosine (RRC) function and the impulse response expressions of the two orthogonal CAP filters [23] in the digital domain are:

$$g_{tx1}[n] = g_{SRRC}[n] \cos(2\pi f_c n) \quad (1)$$

$$g_{tx2}[n] = g_{SRRC}[n] \sin(2\pi f_c n) \quad (2)$$

where n is the sample number, f_c is the digital central frequency of the filter and $g_{SRRC}[n]$ is the RRC function. At the receiver, a pair of filters matched to the transmitter filters are used so the complete response of the filters has the characteristics of the raised cosine (RC) function, which minimizes intersymbol interference (ISI). Fig. 1 shows the CAP modulation scheme

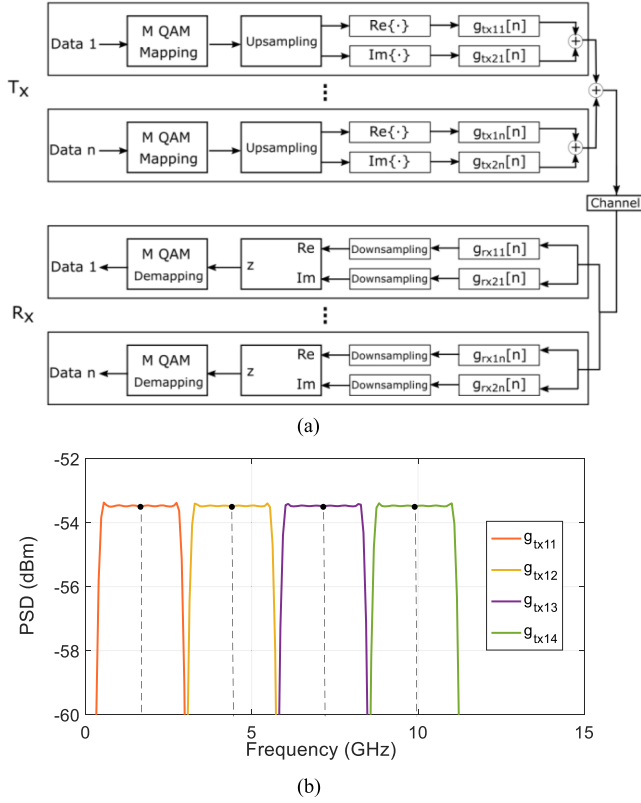


Fig. 2. MultiCAP modulation scheme (a) and frequency response of the MultiCAP filters for a four-band configuration with $\Delta f_{DC} = 400$ MHz, $\beta = 0.1$ and $R_s = 2.5$ Gbaud (b). A sampling rate of $F_s = 80$ GSa/s is assumed in the frequency axis.

and the impulse response of the two orthogonal filters computed with the expressions shown in (1) and (2).

B. Multiband Carrierless Amplitude Phase Modulation

CAP modulation needs a flat frequency response of the whole system to achieve a good performance but this condition is hard to accomplish at high data rates where the signal bandwidth is extended to several GHz. To overcome this limitation, MultiCAP modulation can be used. The idea is to divide the whole spectrum of the CAP signal into several sub-bands and modulate each one of these bands like an independent CAP channel. This technique guarantees a locally flat frequency response on each band and allows using bit- and power-loading techniques independently for each sub-band [24]. From other perspective, the use of different and independent sub-bands allows a flexible resource allocation of different users or services. Fig. 2 shows the MultiCAP modulation scheme and the frequency response of the filters which impulse responses are computed using the following expressions:

$$g_{tx1k}[n] = g_{SRRC}[n] \cos(2\pi f_k n) \quad (3)$$

$$g_{tx2k}[n] = g_{SRRC}[n] \sin(2\pi f_k n) \quad (4)$$

$$f_k = \Delta f_{DC} + \frac{1+\beta}{2} R_s + (R_s + \beta R_s)(k-1) \quad (5)$$

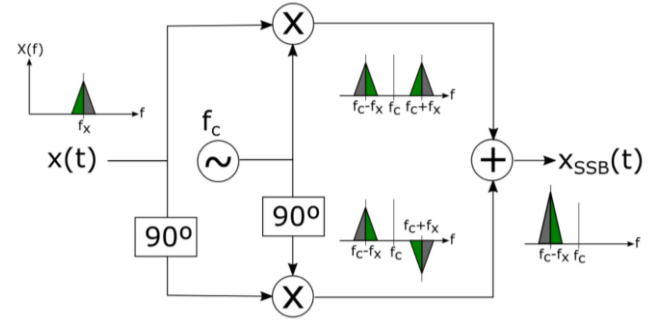


Fig. 3. Single Sideband modulation scheme using the phase shift method.

Where f_k is the digital central frequency of the k -band, $k = 1, \dots, N$ is the band number, Δf_{DC} is the offset of the first band respect to DC, R_s is the symbol rate of each band and β is the roll-off factor of the CAP filters.

C. Optical Single Sideband

When a real baseband signal is used to modulate a carrier, two identical bands appear on the frequency domain, one at each side of the carrier, obtaining a Double Sideband (DSB) modulation that has redundant information in the frequency domain. The SSB modulation takes advantage of this observation to reduce the occupied bandwidth by suppressing one of the two identical bands in DSB. There exist different ways to generate a SSB signal, and in this work we use the phase-shift method [25]. This method, shown in Fig. 3, is based on the combination of two DSB signals generated by modulating two orthogonal carriers with two baseband signals in quadrature. This technique can be applied to any baseband signal, such as the MultiCAP signal presented in section B. In this work, we will digitally generate a MultiCAP baseband signal and calculate its Hilbert transform. Then, these two signals will be applied to the I and Q branches of an optical IQ-modulator to obtain the desired Optical Single Sideband (OSSB) MultiCAP signal with half the bandwidth of the original DSB-MultiCAP signal. From a practical point of view, this technique can be implemented in the analog domain using a 90° hybrid RF coupler instead of using the digital Hilbert transform.

III. EXPERIMENTAL SETUP

The experimental setup used to test the OSSB-MultiCAP system performance is shown in Fig. 4 and the details of this setup are presented in the following sections.

A. Digital Generation of the MultiCAP Signal

The MultiCAP signal has 4 bands, each one presenting a baud-rate of 2.5 GBd, and it is digitally computed using Matlab. For each band, the process shown in the TX part of Fig. 2 is done. First, a pseudo random bit sequence (PRBS) of length 4095 bits (PRBS12) is mapped to a M-QAM constellation. The constellation is varied from 16- to 32-QAM in order to obtain an aggregated bit rate of 40 Gb/s or 50 Gb/s, respectively. Then,

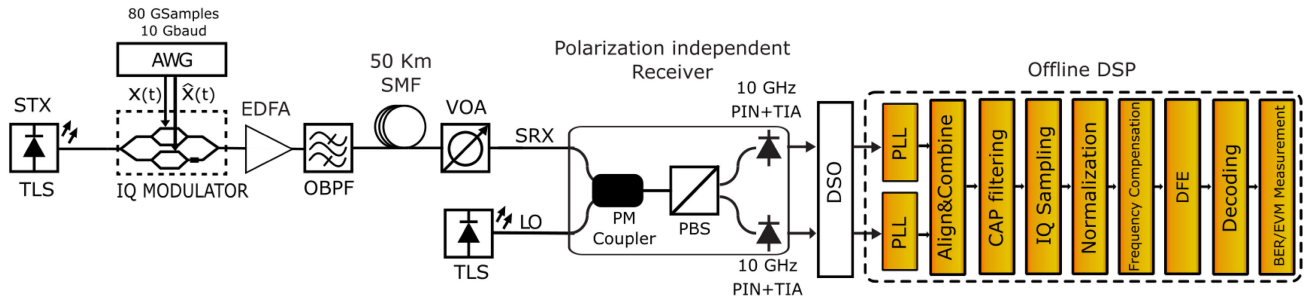


Fig. 4. Schematic of experimental setup. TLS: tunable light source, AWG: arbitrary waveform generator, VOA: variable optical attenuator, SMF: standard single-mode fiber, LO: local oscillator, PM Coupler: polarization mode coupler, PBS: polarization beam splitter, TIA: transimpedance amplifier, DSO: digital storage oscilloscope, DFE: decision feedback equalizer, EDFA: erbium doped fiber amplifier, OBPF: Optical Band Pass Filter.

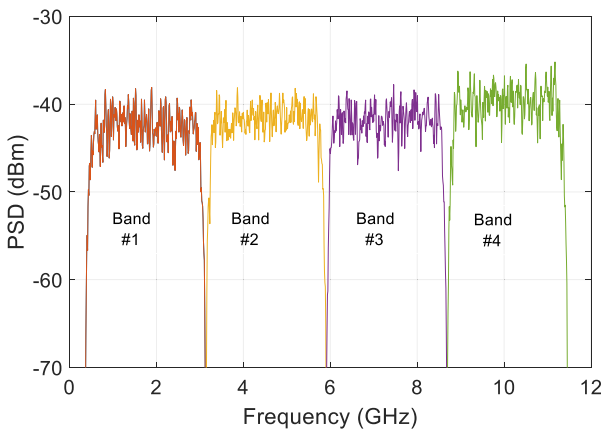


Fig. 5. Digital spectrum of the generated MultiCAP signal, where we have colored the bands for a better differentiation. The variation in power between bands is due to power-loading.

the symbols are up-sampled and filtered using a pair of CAP filters with a length of 50 symbols and a roll-off factor of 0.1. This whole process is repeated for each band, being the central frequency of the filters different for each band following (5) and the first band is separated 400 MHz from DC. Each of the four bands may be weighted and finally all of them are combined, obtaining the actual digital MultiCAP signal. The weighting process is a power-loading mechanism that can compensate the frequency response of the whole system and any impairment between bands in the setup. Although bit-loading techniques can also be implemented with MultiCAP signals, we are not using them in this work because we want to keep the same bit rate for all the bands. The digital spectrum of the obtained MultiCAP signal is shown in Fig. 5, where the power difference between bands is due to the power-loading.

B. Optical Signal Generation

Once the MultiCAP digital signal has been generated, its Hilbert transform is computed and both signals are sent to two different channels of an 80 GSa/s Arbitrary Waveform Generator (AWG). Each channel is electrically amplified and then fed to the I and Q inputs of an optical IQ modulator each of which is biased at its null point. A tunable light source (TLS) centered at 1550 nm is used as the optical source and modulated by

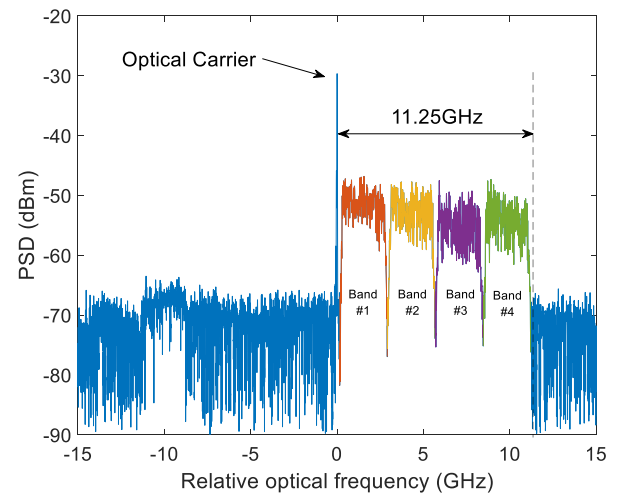


Fig. 6. High resolution optical spectrum of the OSSB-MultiCAP signal centered at 1550 nm. The different bands have been colored for a better discrimination.

the IQ modulator. The obtained OSSB-MultiCAP signal has an optical bandwidth, including the optical carrier and the four bands, of 11.25 GHz. Fig. 6 shows the optical spectrum of the OSSB-MultiCAP measured using a high-resolution optical spectrum analyzer. Each of the four MultiCAP bands is clearly visible in the signal spectrum along with a residual optical carrier due to the finite extinction ratio in the IQ modulator. A sideband optical suppression factor over 20 dB is achieved.

The output of the IQ modulator is coupled to 50 km of standard single mode optical fiber (SSMF) and a variable optical attenuator (VOA). An EDFA may be used after the IQ modulator for boosting the transmitted optical power and to increase the power budget, and its impact on the link performance has been analyzed. A 100 GHz optical band pass filter has been also used to filter out part of the EDFA Amplified Spontaneous Emission (ASE) noise.

C. Coherent Polarization Independent Receiver

At the receiver side, a coherent polarization independent design is used. The received signal is coupled to a 50/50 polarization maintaining optical coupler with a local oscillator (LO) that is another TLS centered at 1550 nm and tuned 11.75 GHz

apart from the optical carrier of the OSSB-MultiCAP signal. The output of the coupler is connected to a polarization beam splitter (PBS) whose outputs are connected a pair of 10 Gb/s PIN+TIA receivers. The LO polarization is aligned to 45 degrees of the PBS axis, so half of its power is in each photodetector. The signal at each detector is digitalized by a Digital Storage Oscilloscope (DSO) at 80 GSa/s and processed offline.

D. Receiver Digital Signal Processing

Once the signals have been digitalized, they are processed offline. First, the two captured signals are time-aligned to compensate for possible impairments in their optical and electrical paths. This step is done computing a windowed cross-correlation of the signals. Then, each signal is down-converted individually using a Phase-Locked Loop (PLL) locked to the residual optical carrier, the two resultant baseband signals are combined and the baseband MultiCAP signal is recovered. This down-conversion is made for the whole MultiCAP signal at once, not for each of the four MultiCAP bands. After that, the combined signal is filtered, for each MultiCAP band, using the matched filters and the symbols are recovered from the maximum energy sampling point. After that, a frequency offset correction algorithm and a decision feedback equalizer (DFE) are applied to the recovered symbols. Then the resultant symbols are recovered and the error vector magnitude (EVM) is computed. Finally, the bits are decoded and the bit error rate (BER) is measured.

IV. EXPERIMENTAL RESULTS

In this section, the results of testing the proposed OSSB-MultiCAP system under different conditions are presented and discussed. First, the performance of the system with an aggregated bit rate of 40 Gb/s is examined for back-to-back (BTB) and 50 km optical fiber links. In this first configuration, we also analyze the use of an Erbium Doped Fiber Amplifier as a booster and the optical power budget will be addressed for this case. Later, the transmission of 50 Gb/s will be also evaluated and compared to the results obtained for 40 Gb/s. Finally, the interference of near or adjacent channels over the transmitted 40 Gb/s link will be studied.

A. 40 Gb/s Links

In the first configuration we use 16-QAM in each band obtaining an aggregated bit rate of 40 Gb/s. In the BTB link, the output of the IQ modulator is connected to the VOA and its output is directly connected to the receiver. Fig. 7 shows the signal spectrum of the 40 Gb/s recovered baseband MultiCAP signal and the received constellations for each band in this BTB link with a received optical power of -15 dBm. It can be seen that the obtained BTB EVM is around 6% for all the bands, being the mean EVM for the four bands 6.625% and the second band the one presenting the worst EVM in this measurement. It can be noticed that, unlike the optical spectrum, all bands have approximately the same power. This is due to power-loading, which allows to equalize the power for all bands

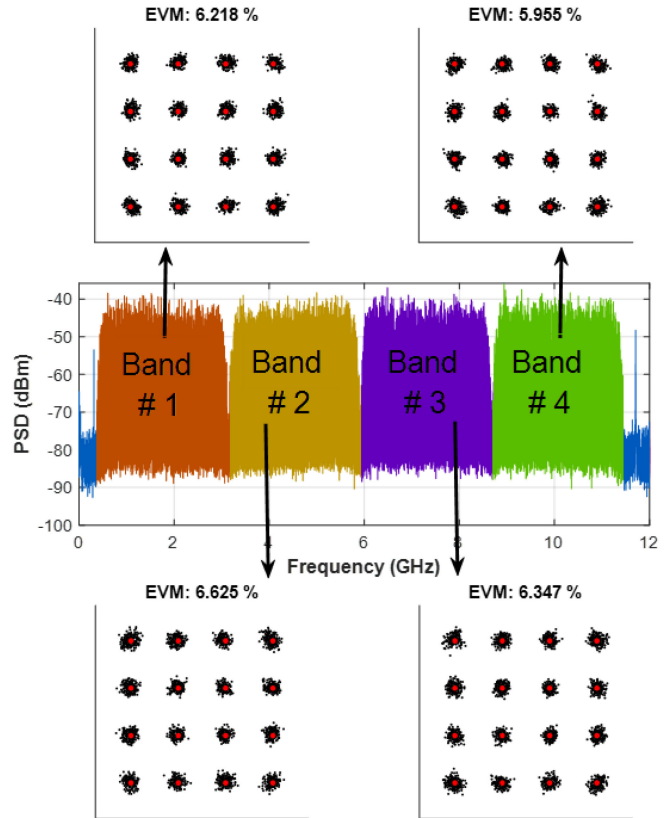


Fig. 7. Signal spectrum of the 40 Gb/s recovered baseband MultiCAP signal and the constellations for each band in the BTB configuration. The different bands have been colored for a better discrimination.

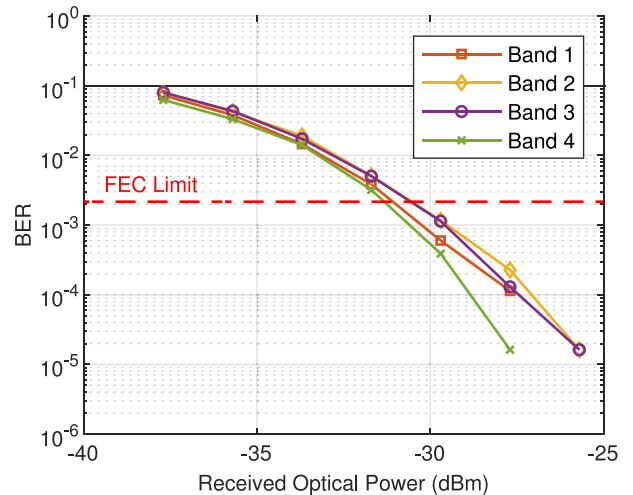


Fig. 8. Bit-error rate for the four MultiCAP bands in BTB configuration with an aggregated data-rate of 40 Gb/s

and to compensate for any optical or electrical impairment, thus obtaining a similar EVM value for all bands.

Fig. 8 shows the measured BTB sensitivity curve for each band using the polarization-independent receiver. The achieved minimum sensitivity, defined as the received optical power to ensure the FEC limit of $BER = 2.17 \times 10^{-3}$ in the worse band, is -30.5 dBm.

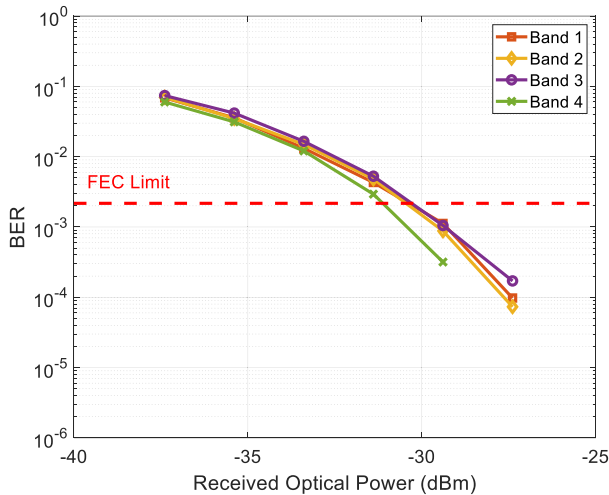


Fig. 9. Bit-error rate for the four MultiCAP bands with unamplified 50 km SSMF at 40 Gb/s.

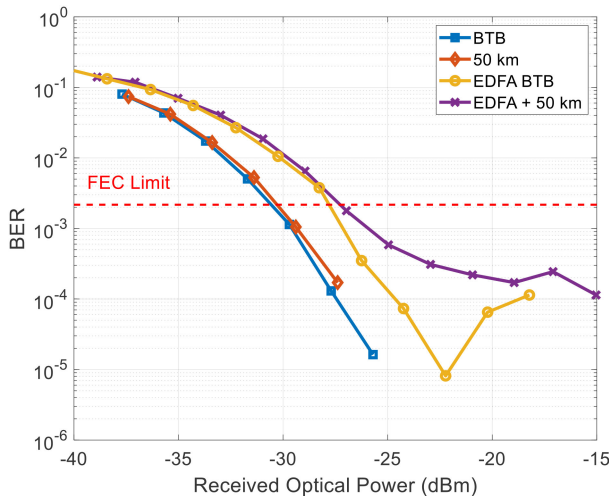


Fig. 10. Bit-error rate for the worst MultiCAP band (third band) for the different configurations at 40 Gb/s.

In the case of 50 km of SSMF, the optical fiber does not introduce any penalty, keeping the sensitivity value in -30.5 dBm, as can be seen in Fig. 9. The measured power budget of this unamplified link is 20.5 dB because the output optical power after the IQ modulator is just -10 dBm. This optical power budget could be increased using an IQ modulator with lower insertion losses or including a booster EDFA before the fiber. The use of EDFA will not only increase the transmitted optical power but may also introduce a penalty in the system sensitivity due to its ASE and non-linear effects in the fiber.

Fig. 10 shows the BER of one MultiCAP band for the different configurations (unamplified and amplified, BTB and 50 km SSMF). Only the worst band, third band in our measurements, has been shown for a clearer view of the system behavior. As it has been predicted, the inclusion of the EDFA not only increases the launching power up to $+5$ dBm but also introduces a penalty in the system sensitivity of about 2.8 dB due to its ASE. In spite

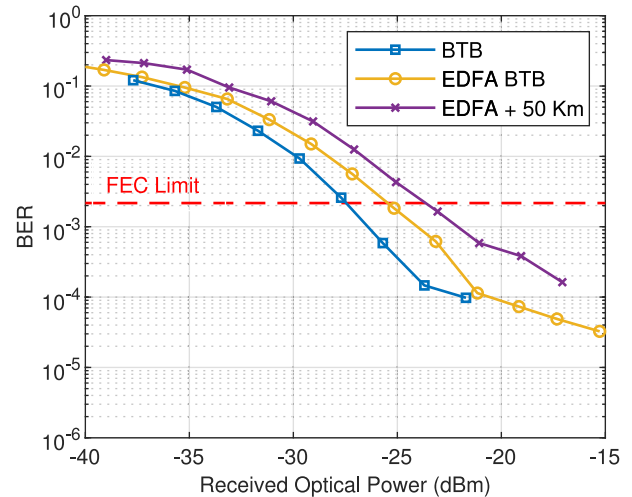


Fig. 11. Bit-error rate for the worst MultiCAP band (third band) for the different configurations at 50 Gb/s.

of this penalty, the optical power budget has been increased from 20.5 dB to at least 32.5 dB for all the bands for 50 km transmission.

B. 50 Gb/s Links

In order to increase the aggregated data rate up to 50 Gb/s, a 32-QAM constellation can be used in each MultiCAP band. In this configuration a minimum sensitivity of -27.5 dBm for the worst band is obtained for the BTB configuration while -23.2 dBm is achieved when using the EDFA and 50 km of SSMF, as is depicted in Fig. 11. It can also be seen from the Fig. that a penalty of about 2 dB is produced when both EDFA and 50 km of SSMF are used respect to the EDFA BTB case. This effect has not been seen for 40 Gb/s links and it is expected to be produced by phase noise induced by the EDFA in the optical fiber. Therefore, the launching optical power for 32-QAM constellations, far more sensitive than 16-QAM ones, needs additional optimization as higher optical powers give rise to higher penalties. Consequently, the optical launching power in the fiber has been adjusted to $+2$ dBm to minimize the penalty due to EDFA phase-noise. However, despite this penalty, this configuration is able to provide a power budget of at least 25.2 dB for all bands for a 50 Gb/s transmission through 50 km SSMF using 10G devices.

C. Adjacent Channel Interference

Finally, an adjacent channel has been added as interfering signal to test the robustness of the received signal and the user channel width requirements in a UDWDM scenario where more users or channels are introduced in the link and filtered by the coherent receptor without using any optical filter or demultiplexer. As shown in Fig. 12, a 10 Gbd (40 Gb/s) DSB-MultiCAP signal, with an optical bandwidth of about 22.5 GHz, is coupled with the OSSB-MultiCAP signal before their injection in the 50 km SSMF.

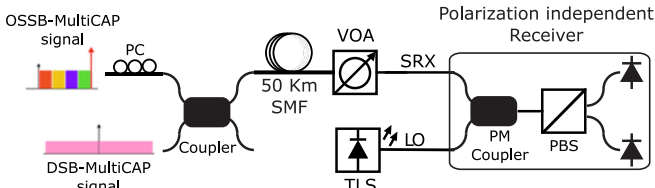


Fig. 12. Experimental setup used in the interference measure.

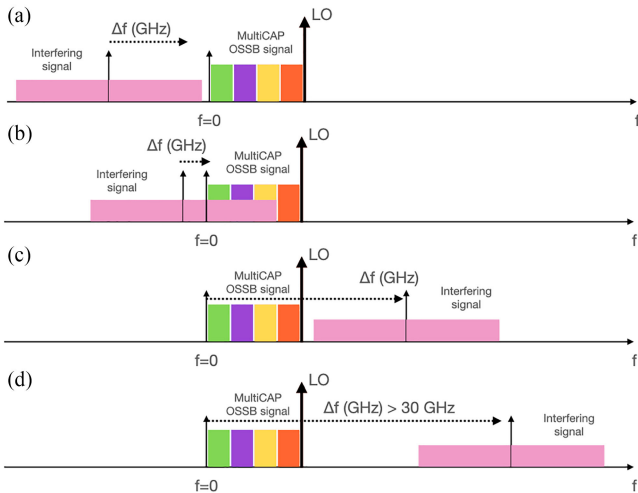


Fig. 13. Frequency spectra of test and interfering signals during the interference process.

The central frequency of the adjacent channel is tuned and Fig. 13 shows the schematic frequency spectra of the interfering and the test signals during the interference measurements. Four different interfering scenarios can be observed depending on the position of the interference signal with respect to the test signal: a) if the central frequency of the interfering signal is more than 10 GHz lower than the optical carrier of the test signal, both signals are not interfering; b) from 10 GHz at lower frequencies respect to the optical carrier to ~ 20 GHz at higher frequencies, both signals share part of the spectrum and hence are interfering; c) from ~ 20 GHz to ~ 30 GHz at higher frequencies, the optical signals are not spectrally overlapped, but the interfering signal is beating with the LO and the interfering electrical signal overlaps the received signal; and d) if the interfering signal is more than ~ 30 GHz higher than the optical carrier, there is no interference at all.

Measured results for each of these scenarios have been depicted in Fig. 14, where BER has been measured for different position of the interfering signal respect to the signal optical carrier frequency. It can be seen that the BER behavior matches with the interference pattern depicted in Fig. 13 and there is a ~ 45 GHz range where the adjacent channel cannot be placed. This interference frequency range could be reduced if the interfering signal was also an OSSB-MultiCAP signal because the used interfering signal spectrum is twice wider than an OSSB one. It is also remarkable that the different bands present different interference behavior. For example, while the interference signal is swept from scenario a) to d) this interference signal arrives first to band 1, but this band is also the last one to interfere

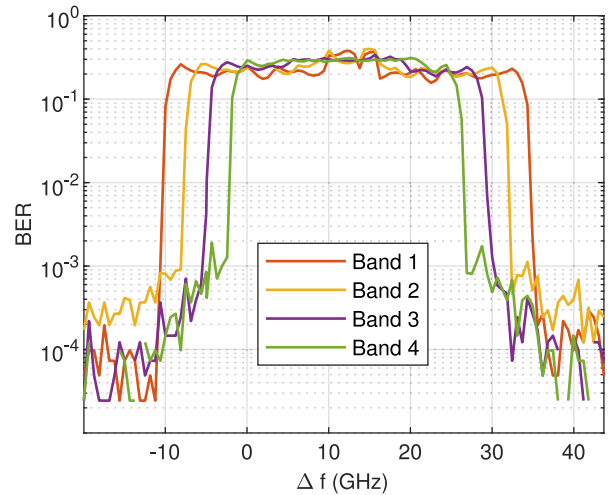


Fig. 14. Interference spectrum of the four MultiCAP bands when a 20 GHz DSB-MultiCAP interference signal is swept across the near bandwidth of the signal. The value of $\Delta f = 0$ corresponds to the optical carrier.

with the signal achieving the maximum interference frequency range. The band 1 is the closest to the optical carrier but is also the farthest band from the LO. On the other hand, band 4 is the one presenting a narrower interference range as it is the one farther from the interference signal at the beginning and it is the first one to exit the interference zone in the scenario c). With these results we can conclude that UDWDM adjacent DSB-MultiCAP channels can be placed with a separation of 45 GHz without penalty in any band and in a scenario with all user channels using OSSB-MultiCAP this separation could be reduced to 22.5 GHz, doubling the number of channels or users and doubling the spectral efficiency of the link.

V. CONCLUSION

The OSSB-MultiCAP modulation scheme has been proposed as a flexible and spectrally efficient per wavelength alternative for next generation high capacity access links. 40 and 50 Gb/s transmission over 50 km of SSMF has been experimentally demonstrated using only 10G electronic and photonic devices and 4×2.5 GBd MultiCAP bands employing a total optical bandwidth of 11.25 GHz. The proposed system is also polarization independent and avoids polarization related issues usually found in coherent receivers. The achieved sensitivity for the worst band was -27.5 dBm for the 40 Gb/s case and -23.2 dBm for the 50 Gb/s case, whereas the measured power budgets were 32.5 dB and 25.2 dB, respectively (always for the worst band). These budgets allow a split ratio of 1:32 for a 50 km, 50 Gb/s case, which may be higher for shorter distances, and up to 1:128 for the 50km, 40 Gb/s case. We have experimentally seen that the use of an EDFA to increase the optical power budget, introduces noise that degrades the OSSB-MultiCAP signal and hence the sensitivity of the system in 2.5 dB. It has also been shown that here is no additional penalty when introducing 50 km of SSMF with respect to the BTB case for 16-QAM (40 Gb/s) transmission, while for the 32-QAM (50 Gb/s) case a penalty of about 2 dB has been measured, suggesting that higher

modulation orders are more sensitive to the effects of phase noise due to the introduction of the EDFA.

REFERENCES

- [1] D. Nessel, "NG-PON2 technology and standards," *J. Lightw. Technol.*, vol. 33, no. 5, pp. 1136–1143, Mar. 2015, doi: [10.1109/jlt.2015.2389115](https://doi.org/10.1109/jlt.2015.2389115).
- [2] D. Zhang, D. Liu, X. Wu, and D. Nessel, "Progress of ITU-T higher speed passive optical network (50G-PON) standardization," *J. Opt. Commun. Netw.*, vol. 12, no. 10, pp. D99, Jun. 2020, doi: [10.1364/jocn.391830](https://doi.org/10.1364/jocn.391830).
- [3] X. Liu and F. Effenberger, "Emerging optical access network technologies for 5G wireless," *J. Opt. Commun. Netw.*, vol. 8, no. 12, pp. B70, Nov. 2016, doi: [10.1364/jocn.8.000b70](https://doi.org/10.1364/jocn.8.000b70).
- [4] F. J. Effenberger, "PON standardisation status and future prospects," in *Proc. 45th Eur. Conf. Opt. Commun.*, 2019, pp. pp. 1–pp. 3, doi: [10.1049/cp.2019.0793](https://doi.org/10.1049/cp.2019.0793).
- [5] Huawei, "50G PAM4 technical white paper," [Online]. Available: <https://carrier.huawei.com/~media/CNDBGV2/download/products/networks/50G-PAM4-Technical-White-Paper.pdf>
- [6] S. Yin, V. Houtsuma, D. van Veen, and P. Vetter, "Optical amplified 40-Gbps symmetrical TDM-PON using 10-Gbps optics and DSP," *J. Lightw. Technol.*, vol. 35, no. 4, pp. 1067–1074, Feb. 2017, doi: [10.1109/jlt.2016.2614767](https://doi.org/10.1109/jlt.2016.2614767).
- [7] J. Wei and E. Giacomidis, "Multi-band CAP for next-generation optical access networks using 10-G optics," *J. Lightw. Technol.*, vol. 36, no. 2, pp. 551–559, Jan. 2018, doi: [10.1109/jlt.2017.2772894](https://doi.org/10.1109/jlt.2017.2772894).
- [8] A. J. Lowery, "Amplified-spontaneous noise limit of optical OFDM lightwave systems," *Opt. Exp.*, vol. 16, no. 2, pp. 860, 2008, doi: [10.1364/oe.16.000860](https://doi.org/10.1364/oe.16.000860).
- [9] M. Xu, J. Shi, J. Zhang, J. Yu, and G.-K. Chang, "High-Capacity Tier-II fronthaul network with SSB-DD multiband OQAM/QAM-CAP," in *Proc. Eur. Conf. Opt. Commun.*, 2017, pp. 1–3, doi: [10.1109/ecoc.2017.8346012](https://doi.org/10.1109/ecoc.2017.8346012).
- [10] Y. Zeng *et al.*, "A novel CAP-WDM-PON employing multi-band DFT-Spread DMT signals based on optical hilbert-transformed SSB modulation," *IEEE Access*, vol. 7, pp. 29397–29404, 2019.
- [11] Z. Dong, J. Yu, and J. Lu, "Bandwidth-Efficient WDM-CAP-PON using digital hilbert single-sideband modulation," *IEEE Photon. J.*, vol. 7, no. 5, pp. 1–7, Oct. 2015, doi: [10.1109/jphot.2015.2480543](https://doi.org/10.1109/jphot.2015.2480543).
- [12] A. Mecozzi, C. Antonelli, and M. Shtaif, "Kramers–Kronig coherent receiver," *Optica*, vol. 3, no. 11, pp. 1220, Oct. 2016, doi: [10.1364/optica.3.001220](https://doi.org/10.1364/optica.3.001220).
- [13] Z. Li *et al.*, "Joint optimisation of resampling rate and Carrier-to-Signal power ratio in direct-detection kramers-kronig receivers," in *Proc. Eur. Conf. Opt. Commun.*, 2017, pp. 1–3, doi: [10.1109/ecoc.2017.8346206](https://doi.org/10.1109/ecoc.2017.8346206).
- [14] M. S. Erkilinc *et al.*, "Comparison of low complexity coherent receivers for UDWDM-PONs (λ -to-the-User)," *J. Lightw. Technol.*, vol. 36, no. 16, pp. 3453–3464, Aug. 2018, doi: [10.1109/JLT.2018.2835376](https://doi.org/10.1109/JLT.2018.2835376).
- [15] J. A. Altabas *et al.*, "Real-Time 10 gbps polarization independent quasioherent receiver for NG-PON2 access networks," *J. Lightw. Technol.*, vol. 37, no. 2, pp. 651–656, Jan. 2019, doi: [10.1109/JLT.2018.2880361](https://doi.org/10.1109/JLT.2018.2880361).
- [16] B. Glance, "Polarization independent coherent optical receiver," *J. Lightw. Technol.*, vol. 5, no. 2, pp. 274–276, 1987, doi: [10.1109/jlt.1987.1075494](https://doi.org/10.1109/jlt.1987.1075494).
- [17] M. S. Erkilinc *et al.*, "Polarization-Insensitive single-balanced photodiode coherent receiver for long-reach WDM-PONs," *J. Lightw. Technol.*, vol. 34, no. 8, pp. 2034–2041, Apr. 2016, doi: [10.1109/jlt.2015.2507869](https://doi.org/10.1109/jlt.2015.2507869).
- [18] J. A. Altabas, O. Gallardo, G. S. Valdecasa, M. Squartecchia, T. K. Johansen, and J. B. Jensen, "DSP-Free real-time 25 GBPS quasioherent receiver with electrical SSB filtering for C-Band links up to 40 km SSMF," *J. Lightw. Technol.*, vol. 38, no. 7, pp. 1785–1788, Apr. 2020, doi: [10.1109/jlt.2019.2963787](https://doi.org/10.1109/jlt.2019.2963787).
- [19] C. Bock, J. M. Fabrega, and J. Prat, "Ultra-Dense WDM PON based on homodyne detection and local oscillator reuse for upstream transmission," in *Proc. 32nd Eur. Conf. Opt. Commun.*, 2006, pp. 1–2, doi: [10.1109/ecoc.2006.4801361](https://doi.org/10.1109/ecoc.2006.4801361).
- [20] M. S. Erkilinc, Z. Liu, T. Gerard, R. I. Killey, P. Bayvel, and D. Lavery, "Bidirectional symmetric 25G coherent ONU using a single laser, single-ended PIN and a 2-bit ADC," in *Proc. Eur. Conf. Opt. Commun.*, 2018, pp. 1–3, doi: [10.1109/ecoc.2018.8535127](https://doi.org/10.1109/ecoc.2018.8535127).
- [21] J. A. Altabas, D. Izquierdo, J. A. Lazaro, and I. Garces, "Cost-Effective transceiver based on an RSOA and a VCSEL for flexible uDWDM networks," *IEEE Photon. Technol. Lett.*, vol. 28, no. 10, pp. 1111–1114, May 2016, doi: [10.1109/lpt.2016.2531789](https://doi.org/10.1109/lpt.2016.2531789).
- [22] A. H. Abdolhamid and D. A. Johns, "A comparison of CAP/QAM architectures," in *Proc. IEEE Int. Symp. Circuits Syst.*, 1998, pp. 316–316/3, doi: [10.1109/iscas.1998.698823](https://doi.org/10.1109/iscas.1998.698823).
- [23] N. M. Ridzuan, M. F. L. Abdullah, M. B. Othman, and M. B. Jaafar, "A carrierless amplitude phase (CAP) modulation format: Perspective and prospect in optical transmission system," *IJECE*, vol. 8, no. 1, pp. 585, Feb. 2018, doi: [10.11591/ijece.v8i1.pp585-595](https://doi.org/10.11591/ijece.v8i1.pp585-595).
- [24] M. I. Olmedo *et al.*, "Multiband carrierless amplitude phase modulation for high capacity optical data links," *J. Lightw. Technol.*, vol. 32, no. 4, pp. 798–804, Feb. 2014, doi: [10.1109/jlt.2013.2284926](https://doi.org/10.1109/jlt.2013.2284926).
- [25] A. Loayssa, D. Benito, and M. J. Garde, "Single-sideband suppressed-carrier modulation using a single-electrode electrooptic modulator," *IEEE Photon. Technol. Lett.*, vol. 13, no. 8, pp. 869–871, Aug. 2001, doi: [10.1109/68.935831](https://doi.org/10.1109/68.935831).